

Growth Processes in a Cascade of Bioreactors: Comparison of Modeling Approaches

Nikolaos V. Mantzaris, Prodromos Daoutidis, Friedrich Srienc, and Arnold G. Fredrickson

Dept. of Chemical Engineering and Materials Science, Biological Process Technology Institute,
University of Minnesota, Minneapolis, MN 55455

The theory of a two-tank cascade of bioreactors developed by Mantzaris et al. (1998) was used to calculate the performance of such a cascade predicted by two chemically structured models: one for gene expression of Bentley and Kompala (1989) and Bentley et al. (1991) and the other a cybernetic model of Kompala et al. (1986) for multiple substitutable substrates. Two modeling approaches developed previously—one that accounts for biomass segregation and one that does not—were used with the model of Bentley and Kompala (1989) and Bentley et al. (1991). These modeling approaches showed that, in general, biomass segregation is an important feature of what happens in the second tank of the cascade and cannot be neglected. The same two approaches as well as a third approach based on the use of a chemically unstructured model were applied to the model of Kompala et al. (1986). It was found that biomass segregation in the second tank was important under some circumstances but not all and that the unstructured model failed to describe accurately what happens in the second tank under all circumstances.

Introduction

The equations and computational methods for using a chemically structured model to predict growth and product formation behavior in each tank of a two-tank cascade of bioreactors were presented in a previous article (Mantzaris et al., 1998). A chemically structured model takes account of the changes in biomass composition which result when the biomass experiences a change in the state of its abiotic environment, and the equations given also take account of the fact that biomass transferred from tank 1 and 2 remains segregated from the other biomass in tank 2. For this reason, the equations referred to are said to be a segregated approach to the problem of describing the dynamics of the bioreactor cascade. Simpler versions of these equations were worked out, also. One version employs a chemically structured model but explicitly ignores segregation of biomass. The equations of this version are said to be an unsegregated approach to the cascade problem. A second version assumes that current biomass specific growth and nutrient uptake rates are functions only of the current state of the biomass envi-

ronment. Since composition structure is irrelevant in this case, the equations are said to be an unstructured approach to the problem of the cascade. Such unstructured approaches have been applied to the cascade system many times in the past.

In this article, the effects of biomass segregation on biomass behavior are investigated by comparing the results of the segregated and unsegregated approaches for the second tank of a cascade when a common chemically structured model is used for both. Similarly, the effects of the existence of internal structure on biomass behavior are investigated by comparing the results of the segregated and unstructured approaches for the second tank. These comparisons are made for two different chemically structured models taken from the literature.

In a real-world application of the theory presented here one would make a detailed examination of the effects of system operating parameters—flow rates, reactor volumes, and feed compositions—on the predicted behavior of the system in order to find out what are the optimum values of the operating parameters. However, one can make the comparisons described in the previous paragraph with only minimal exam-

Correspondence concerning this article should be addressed to A. G. Fredrickson.

ination of the effects of operating parameters on system performance, and so no systematic and extensive examination of such effects has been made.

Choice of a Chemically Structured Model for Use in Illustrative Examples

A chemically structured model that would be ideal for illustrating the theory developed in the foregoing paragraphs should be realistic in the sense that it has been tested by at least some experimentation in apparatus such as batch, single CSTR, and fed-batch, and found to give a reasonably good representation of the data obtained. In addition, it should be a model of growth and product formation by an organism for which there is some obvious practical advantage to be gained by using multiple bioreactors. A model for protein expression by a recombinant organism published by Bentley and Kompala (1989) and Bentley et al. (1991) meets these requirements and it will be used for our first illustrative example.

We shall also present a second illustrative example which is based on a model published by Kompala et al. (1986). This is a so-called cybernetic model and its authors tested it on batch growth of *Klebsiella oxytoca* on mixtures of glucose and one or two other sugars; the model successfully handled diauxic and triauid and related phenomena. There is no obvious practical reason why one would want to grow this organism in a two-tank apparatus, but there are two reasons for including an example based on this model in this article. First, the only way to construct the unstructured model corresponding to the structured model of Bentley and Kompala (1989) is by statistical curve-fitting, which we prefer not to do. The unstructured model corresponding to the model of Kompala et al. (1986) can be constructed analytically, and, therefore, this model can be used to see how the predictions of the unstructured model compare with those of the structured model. Second, mathematical analysis of the model of Bentley and Kompala (1989) would seem to have to be by brute force numerical methods, but analytical methods can be used, at least to some extent, to investigate the nonlinear features of the model of Kompala et al. (1986).

First Example: Model Describing the Dynamics of Induced Protein Expression

Bentley and Kompala (1989) proposed a structured kinetic model for the dynamics of induced chloramphenicol-acetyl transferase (CAT) expression in *Escherichia coli*. The kinetics of the inducer (isopropyl- β -D-thiogalactopyranoside (IPTG)) transport were later added to the model by Bentley et al. (1991). The state vector of the biomass in the complete version of the model has nine elements, and they are the mass fractions of amino acids, nucleotides, lipids, RNA, DNA, protein, foreign protein (CAT), foreign DNA (which encodes for CAT expression), and intracellular inducer in the biomass. The state vector of the abiotic environment has two elements, and they are concentrations of the substrate (LB) and the extracellular inducer. The model parameter values used in all simulations were those given by Bentley and Kompala (1989) and Bentley et al. (1991). In all of the simulation results that will be presented, it was assumed that the cascade

of two CSTRs shown in Figure 1 of the previous article (Mantzaris et al., 1998) is used, that inducer is present in the feed to the second reactor but not in the feed to the first reactor, and that there is perfect plasmid (foreign DNA) stability in both reactors. Operating parameters used in all the simulations to be presented were as follows (refer to the aforementioned figure): $D_1 \equiv Q_1/V_1 = 1.5 \text{ h}^{-1}$, $\phi \equiv Q_1/(Q_1 + Q_2) = 0.5769$, $D_2 \equiv (Q_1 + Q_2)/V_2 = 2.6 \text{ h}^{-1}$, $(s_{1f})_{LB} = 2 \text{ kg} \cdot \text{m}^{-3}$, $(s_{2f})_{LB} = 2 \text{ kg} \cdot \text{m}^{-3}$, and $(s_{1f})_{IPTG} = 0$. Steady-state simulations were done for various values of $(s_{2f})_{IPTG}$ ranging from 1 to 100 mM (0.238 to 23.8 $\text{kg} \cdot \text{m}^{-3}$). A single transient calculation was done using a value of $(s_{2f})_{IPTG} = 10 \text{ mM}$ and all of the other parameters given above. The dilution rate of 1.5 h^{-1} for the first tank is that which maximizes the biomass productivity of that tank when it is operated in steady state with the feed composition given. The dilution rate of 2.6 h^{-1} and the feed fraction ϕ for the second tank are the values that come close to maximizing steady-state CAT productivity of the second tank if: (1) the first tank is operated at the conditions stated; (2) the feed concentrations of LB are those stated and the feed concentration of IPTG to the second tank is 10 mM; (3) the two tanks are of equal volume; and (4) segregation of biomass in the second tank can be neglected and the steady-state productivity calculated by solving the algebraic equations of the unsegregated approach rather than the differential equations of the segregated approach. The latter assumption was made in order to obtain an initial estimate of the optimal values of D_2 and ϕ when the feed concentrations are the stated ones. The choice of $(s_{2f})_{IPTG} = 10 \text{ mM}$ for making this estimate is purely arbitrary.

First Example: Steady-State Simulations

The steady-state behavior of the system was investigated using both the segregated and unsegregated modeling approaches for several different values of the IPTG concentration at the feed of the second reactor, ranging from 1 mM up to 100 mM and for the values of the operating parameters chosen above.

Figure 1 shows the comparison between the two modeling approaches for the second reactor at steady state and as a function of the inducer concentration in the fresh feed to the second reactor. For the case of the segregated approach, the average values of the quantities are shown. Notice that the intracellular inducer and CAT mass fractions, as well as the CAT productivity reach a maximum at a feed inducer concentration of approximately 9 mM. At the same value of feed inducer concentration, the lipid, RNA, DNA, and protein mass fractions reach a minimum. The amino acid and nucleotide mass fractions and the biomass concentration do not show extrema but rather decrease with increase of the feed inducer concentration, whereas the substrate concentration and DNA coding for CAT production increase as the feed inducer concentration is increased. The patterns predicted by the unsegregated approach are similar. However, the values of the feed inducer concentration where extrema are exhibited are different and higher for the unsegregated approach; the maximizing feed inducer concentration is about 13 mM. The results indicate that the unsegregated approach underestimates the substrate concentration, and the amino acid, nu-

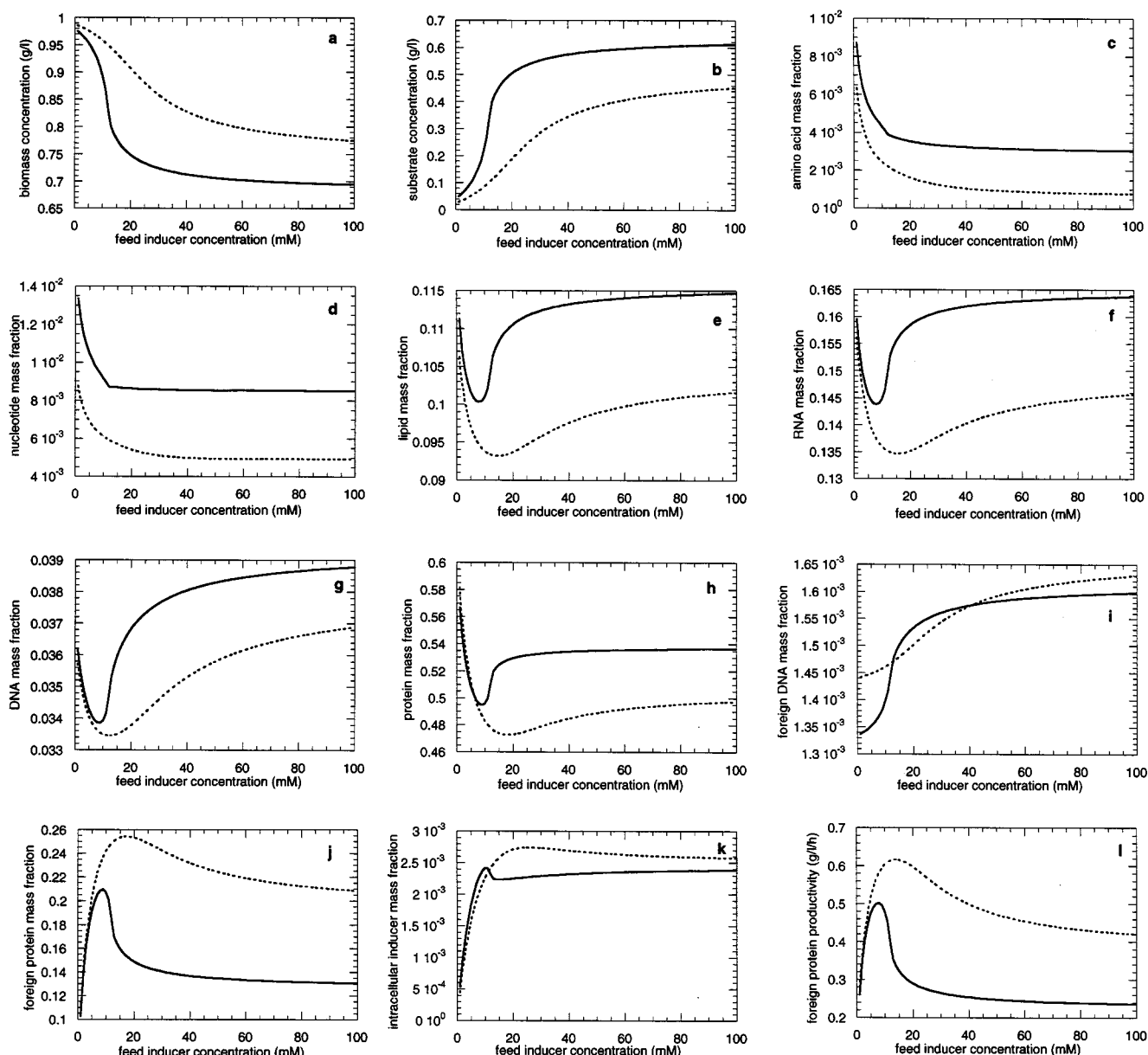


Figure 1. Model of Bentley and Kompala (1989) and Bentley et al. (1991): steady-state results for the second reactor.

It is a function of the concentration of the inducer in the fresh feed to the second reactor, as predicted by the two modeling approaches for $D_1 = 1.5 \text{ h}^{-1}$, $D_2 = 2.6 \text{ h}^{-1}$, $\phi = 0.5769$, $(s_1 \rho)_{LB} = 2 \text{ kg} \cdot \text{m}^{-3}$, $(s_2 \rho)_{LB} = 2 \text{ kg} \cdot \text{m}^{-3}$, $(s_1 \rho)_{IPTG} = 0$. —: Average values predicted by the segregated approach; ---: predictions of the unsegregated approach. (a) Biomass concentration; (b) substrate concentration; (c) amino acid mass fraction; (d) nucleotide mass fraction; (e) lipid mass fraction; (f) RNA mass fraction; (g) DNA mass fraction; (h) protein mass fraction; (i) DNA coding for CAT expression (foreign DNA) mass fraction; (j) CAT (foreign protein) mass fraction; (k) intracellular inducer mass fraction; (l) CAT (foreign protein) productivity.

cleotide, lipid, RNA, DNA, and protein mass fractions, whereas it overestimates the biomass concentration and the CAT mass fraction and productivity over the entire range of feed inducer concentrations.

Figure 2 shows the steady-state distributions with respect to age of the biomass concentration and the mass fractions of DNA, DNA responsible for CAT expression, protein, CAT, and intracellular inducer in the second tank for various values of the feed inducer concentration. Of course, these are

predictions of the segregated approach; the unsegregated approach has nothing to say about distributions with respect to age. Notice that all profiles are qualitatively the same for values of the feed inducer concentration above 50 mM. However, the shape of the profiles is significantly influenced by the feed inducer concentration at lower values. Of particular interest is that, at the feed inducer concentration of 10 mM, which is near optimal for CAT productivity, "old" biomass in the second reactor attains foreign protein contents of more

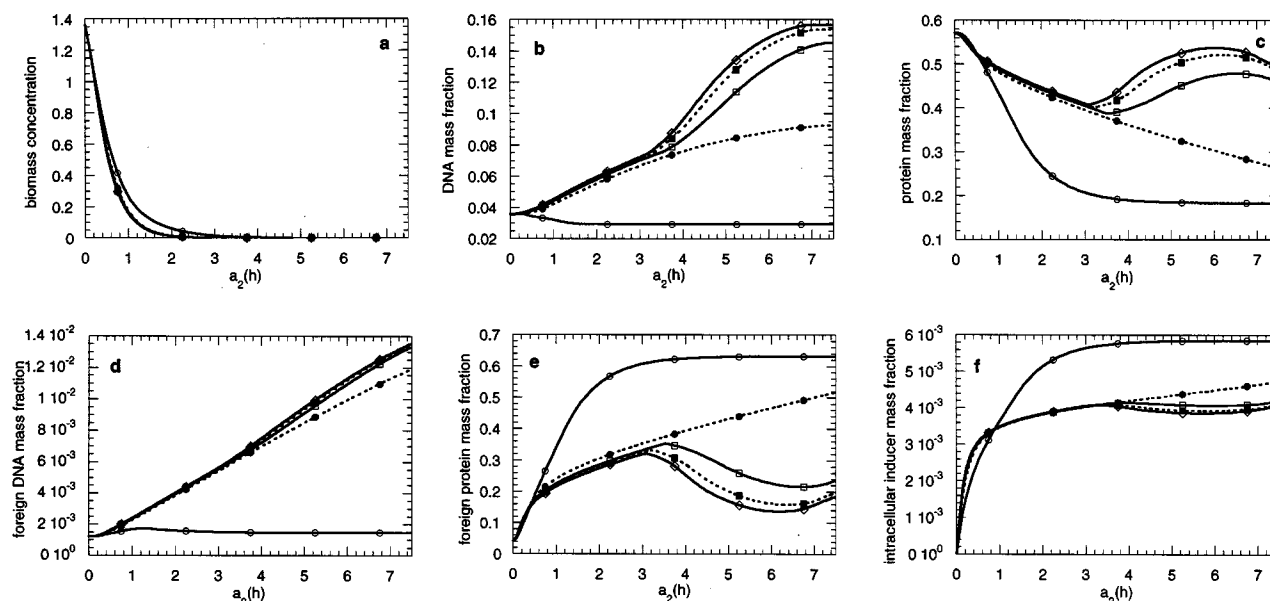


Figure 2. Model of Bentley and Kompala (1989) and Bentley et al. (1991): steady-state age distributions in the second reactor.

It was predicted by the segregated approach, for different values of the concentration of the inducer in the fresh feed to the second reactor. Inducer concentrations: $\circ-\circ-\circ$: 10 mM; $\bullet-\bullet-\bullet$: 30 mM; $\square-\square-\square$: 50 mM; $\blacksquare-\blacksquare-\blacksquare$: 70 mM; $\diamond-\diamond-\diamond$: 90 mM. (a) Biomass concentration; (b) DNA mass fraction; (c) protein mass fraction; (d) DNA coding for CAT (foreign protein) mass fraction; (e) CAT (foreign protein) mass fraction; (f) intracellular inducer mass fraction.

than 60% by weight. Unfortunately, there is very little "old" biomass in the reactor, so that the average foreign protein content of the biomass is only about 20%.

First Example: A Transient Simulation

Figure 3 shows the results of a transient simulation for the second reactor for 10 mM inducer concentration in the feed stream of the second reactor and for the same values of the rest of the operating parameters that were used in the steady-state calculations. Again, the average values of the mass fractions predicted by the segregated approach have been plotted.

Examination of the curves for the segregated approach shows that they have reached asymptotic values after about 4 h from startup. The asymptotic values of the variables are in good agreement with the steady-state value shown in Figure 1 for a feed inducer concentration of 10 mM. Such agreement is a necessary condition for the validity of the numerical calculations done to produce the two sets of figures. Careful examination of the curves for the unsegregated approach shows that several of them have not yet reached asymptotic values as late as 6 h after startup, and this is, of course, a difference between the two modeling approaches. It is obvious that there are other differences, as well, but it can be seen that the differences between the two modeling approaches as applied to the transient situation are consistent with the differences between the approaches reported above for the steady-state situation. Notice that for this value of the feed inducer concentration, neglecting biomass segregation results in overestimating the asymptotic CAT mass fraction and productivity by approximately 25%.

Comments on First Example

The results of the comparison between the two approaches strongly depend on the choice of the operating parameters. Several simulations that were performed for different sets of operating parameters have revealed larger or smaller differences between the two approaches than the ones presented in Figure 1. Moreover, the results of the comparison are influenced by the choice of operating parameters in a qualitative way, as well. For example, for other sets of operating parameters, it was seen that the unsegregated approach consistently underestimates the biomass concentration and overestimates the substrate concentration, over a large range of feed inducer concentrations, contrary to the situation presented in Figure 1. In fact, examination of a large number of simulations like those shown in Figure 1 has not suggested any general conclusion about domains of operating conditions where the differences between the predictions of the two approaches are small or where they are large. In Figure 1, the differences between the predictions of the approaches for *some* of the variables are small when the feed inducer concentration is low. This is to be expected, as when this concentration is low, the environmental shock received by the cells when they are transferred from the first to the second tank is minimal. However, even this weak statement cannot be taken as a generally valid conclusion.

Second Example: A Cybernetic Model

Kompala et al. (1986) have constructed a cybernetic model to describe the batch growth dynamics of *Klebsiella oxytoca* on mixtures of glucose and one or two other sugars. The authors determined the parameters of the model from experi-

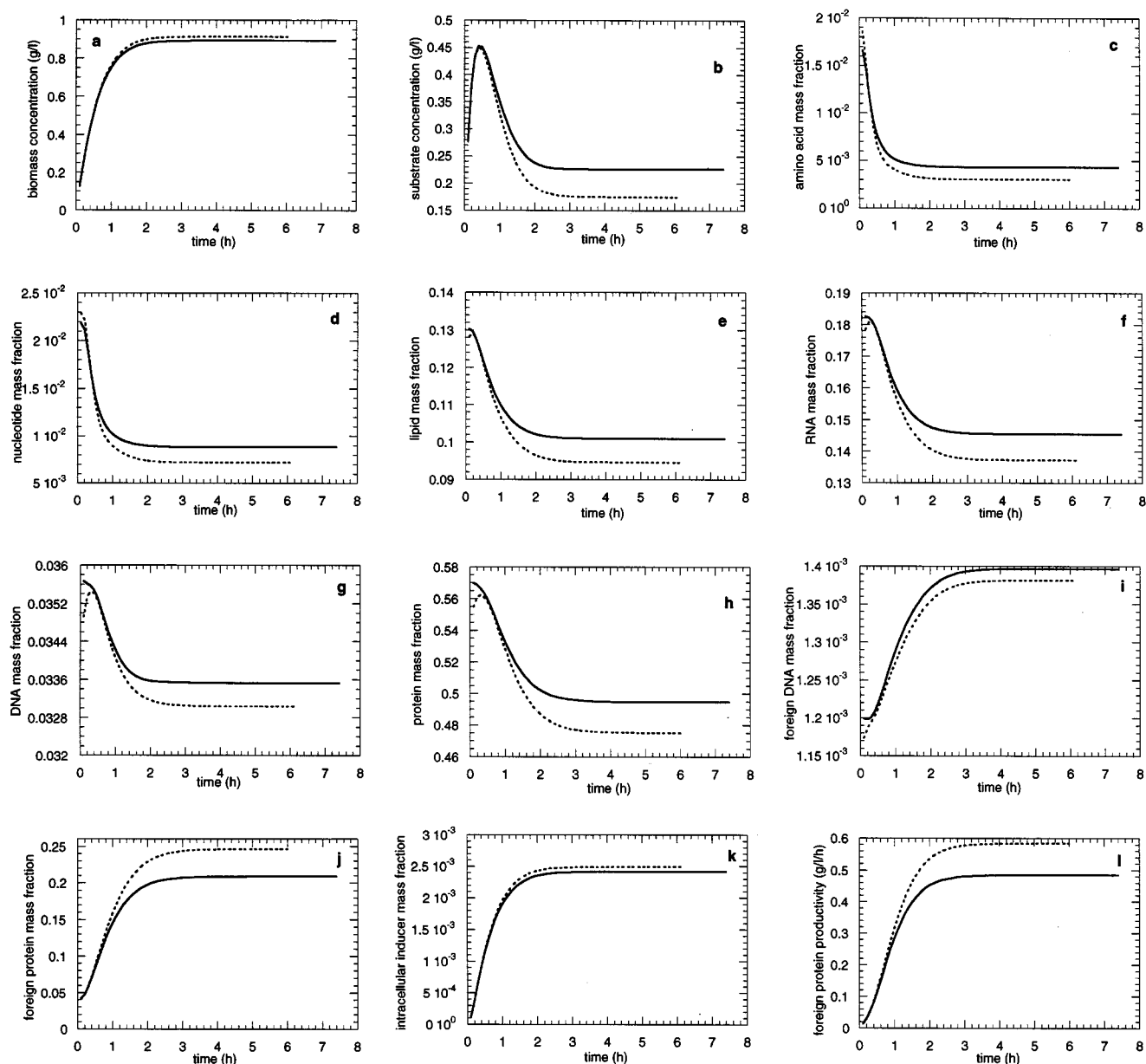


Figure 3. Model of Bentley and Kompala (1989) and Bentley et al. (1991): transient simulation for the second reactor.

It was predicted by the two modeling approaches for the second reactor and for $D_1 = 1.5 \text{ h}^{-1}$, $D_2 = 2.6 \text{ h}^{-1}$, $\phi = 0.5769$, $(s_{1P})_{LB} = 2 \text{ kg} \cdot \text{m}^{-3}$, $(s_{2P})_{LB} = 2 \text{ kg} \cdot \text{m}^{-3}$, $(s_{1P})_{IPTG} = 0$, $(s_{2P})_{IPTG} = 10 \text{ mM}$. —: the average values predicted by the segregated approach; ---: predictions of the segregated approach. (a) Biomass concentration; (b) substrate concentration; (c) amino acid mass fraction; (d) nucleotide mass fraction; (e) lipid mass fraction; (f) RNA mass fraction; (g) DNA mass fraction; (h) protein mass fraction; (i) DNA coding for CAT expression (foreign DNA) mass fraction; (j) CAT (foreign protein) mass fraction; (k) intracellular inducer mass fraction; (l) CAT (foreign protein) productivity.

ments in which the cells grew on a single sugar, and they showed that the model handled diauxie and triauxie and related phenomena successfully. There is no obvious practical reason why one would want to grow this organism in a two-tank cascade, but we found that application of the model to the two-tank cascade was an excellent way to achieve some of the primary objectives of our research. Although the model is highly nonlinear, it was possible to investigate the steady-state versions of the equations analytically in great depth. This, in turn, allowed the analytical examination of the asymptotic

behavior of the reactor system as a function of the operating parameters of the system (bifurcation analysis). Finally, manipulations of the steady-state version of the model equations enabled us to construct the unstructured version of the model analytically, so that it was possible to compare the predictions of the unstructured version of the model with those of the segregated version.

A complete description of the model of Kompala et al. (1986) and a listing of the model parameters is given in their article, and so these will not be repeated here. Referring to

Figure 1 of the previous article (Mantzaris et al., 1998), we assumed that $Q_2 = 0$ and $V_1 = V_2$ so that $\phi = 1$ and $D_1 \equiv Q_1/V_1 = (Q_1 + Q_2)/V_2 \equiv D_2$. Insofar as substrates are concerned, we assumed that the feed to the first reactor contained glucose and xylose but no other sugars. The number of operating parameters is thus three and they are $D_1 = D_2 \equiv D$ and the concentrations of glucose and xylose in the feed to the first reactor $(s_{1f})_{Glu}$ and $(s_{1f})_{Xyl}$, respectively. The state vectors of the abiotic environment and the biomass contain two and three elements, respectively. The two elements of the abiotic state vector are the aforementioned concentrations of glucose and xylose. Two of the three elements of the state vector of the biomass are the mass fractions of the enzyme systems that metabolize glucose and xylose, and the third is the mass fraction of the rest of the biomass. Since the sum of the mass fractions is 1, only two of the elements are independent, and we choose these to be the mass fractions of the two enzyme systems.

Second Example: Steady-State Analyses

A detailed steady-state analysis for both reactors was performed with the following goals in mind: (a) to find all possible steady states for a given set of operating parameters (D , $(s_{1f})_{Glu}$, and $(s_{1f})_{Xyl}$); (b) to characterize their local asymptotic stability properties using linear stability analysis; and (c) to examine how the number and asymptotic stability of these steady states change as the three operating parameters vary in the parameter space.

Due to the nonlinearity of the steady-state equations for all three approaches and for both reactors, it is possible to have more than one steady-state solution for a given set of operating parameters. For this particular example, and irrespective of the reactor under consideration, one can qualitatively identify five possible types of steady states: (a) a washout steady state where no biomass is produced and neither of the substrates is consumed; (b) a steady state where only glucose is consumed; (c) a steady state where only xylose is consumed; (d) a steady state where both substrates are consumed, but biomass grows mainly on glucose; (e) a steady state where both substrates are consumed but biomass grows mainly on xylose. One can distinguish between the last two types of steady states by comparing the relative magnitude of the rates of biomass production due to the consumption of the two substrates (see Kompala et al., 1986). It is also possible to have a steady state where both substrates are equally consumed. However, this type of steady state can be thought of as a subcase of the (d) and/or (e) types of steady states. It must also be noted that, in principle, it is possible to have more than one steady state of the same type.

Each possible steady-state solution must fall within physically and biologically acceptable limits. For example, the values of the steady-state biomass concentration, substrate concentrations and state vector elements cannot be less than zero. Moreover, the steady-state substrate concentrations in tank 1 cannot be more than the corresponding feed substrate concentrations, and the steady-state substrate concentrations in tank 2 cannot be more than the corresponding steady-state values in tank 1. Hence, the steady-state solution is subject to *constraints*. The application of these constraints to the steady-state solutions of tank 1 has led to the isolation of a

large region in the feed substrate concentration parameter subspace $((s_{1f})_{Glu}, (s_{1f})_{Xyl})$, where the dependence of the number and stability properties of the steady states on the dilution rate D remains *qualitatively* the same. In other words, for any pair $((s_{1f})_{Glu}, (s_{1f})_{Xyl})$ which belongs to this isolated subspace, the steady-state bifurcation diagrams for both reactors, with the dilution rate as the bifurcating parameter, remains qualitatively the same. The upper and lower bounds of this $((s_{1f})_{Glu}, (s_{1f})_{Xyl})$ subspace were analytically found as functions of the model parameters which were taken to be identical to the values given in the article of Kompala et al. (1986). A complete bifurcation analysis was performed for the entire region of dilution rates. The upper bound of this dilution rate region was chosen to be the value above which the only existing steady-state solution for tank 1 is the washout steady state. This upper bound was analytically found as a function of the two feed substrate concentrations and the model parameters.

In all the simulations and results that will be presented in the following the two feed substrate concentrations were taken to be $(s_{1f})_{Glu} = (s_{1f})_{Xyl} = 0.33 \text{ kg} \cdot \text{m}^{-3}$. These numerical values belong to the isolated region in the feed substrate concentration parameter subspace mentioned above. Given these two values and the model parameters, the upper bound for the dilution rate was found to be $D_u = 1.045 \text{ h}^{-1}$.

Second Example: Determination of Specific Growth Rate and Nutrient Uptake Functions for Unstructured Model

The determination of the specific growth rate and nutrient uptake functions for the unstructured model which corresponds to the structured model proposed by Kompala et al. (1986) was achieved by requiring that these functions are such that they make the same predictions about the biomass and substrate concentrations for steady-state growth in a single CSTR that the structured model makes. According to the structured model, these three functions depend on the two substrate concentrations *and* on the two states. In order to find the corresponding functions for the unstructured model which must depend *only* on the two substrate concentrations, the steady-state equations for the structured model and for the first tank were used.

Although it is not possible to find all steady states in tank 1 analytically, it is *analytically* possible to express the steady-state values of the elements of the state vector as functions of the dilution rate and the two steady-state substrate concentrations for all of the possible steady states mentioned above. Since, at steady state for the first tank, the dilution rate must be equal to the specific growth rate, these expressions give the state vector as a function of the specific growth rate and the substrate concentrations. These expressions were subsequently substituted into the equation defining the specific growth rate for the structured model, which, consequently, no longer contains the state vector. The resulting equation was then analytically solved for the specific growth rate, thus producing the desired function $\mu_{uns}(s)$. Moreover, the equations which give the steady-state values of the states as functions of the specific growth rate and the two substrate concentrations were also substituted in the equations which define the two specific rates of nutrient uptake. Using the pre-

viously derived expression for $\mu_{uns}(s)$, these substitutions yield the corresponding unstructured vector function of nutrient uptake $r_{uns}(s)$. The same functions were used for all the simulations and for both reactors.

Second Example: Steady-State Simulations

The equations which describe the steady-state situation in the first tank are identical for both the segregated and unsegregated approaches and, therefore, the two approaches are identical in this case. The results of simulations in which every parameter except dilution rate was kept constant are shown in Figure 4. The steady-state concentrations of biomass, glucose, and xylose and the mass fractions of the glucose and xylose utilizing enzyme systems in the biomass have been plotted as functions of the dilution rate. Values of these parameters for stable steady states are plotted as solid lines and values for unstable steady states are plotted as dotted lines. By definition, the unstructured approach yields the stable steady-state results in every case.

A detailed bifurcation analysis of these equations with the dilution rate as the bifurcation parameter revealed the existence of a critical dilution rate value D_{cr} which divides the dilution rate space into two regions. For low dilution rates ($D < D_{cr}$), there exist five steady states: (1) a washout steady state where the enzymes that metabolize xylose are not present; (2) a washout steady state where the enzymes that metabolize glucose are not present; (3) a nonwashout steady state where only glucose is consumed; (4) a nonwashout steady state where only xylose is consumed; and (5) a nonwashout steady state where both substrates are consumed but biomass grows mainly on glucose. On the other hand, for high dilution rates ($D > D_{cr}$) only the first three steady states exist.

Moreover, linear stability analysis performed on the entire dilution rate space showed that for any dilution rate only one of the existing steady states is locally asymptotically stable. The rest of the existing steady states are unstable saddles with a single positive eigenvalue. For $D < D_{cr}$, the asymptotically stable steady state is steady state (5), whereas for $D > D_{cr}$, steady state (3) is the single asymptotically stable steady state. Thus, at $D = D_{cr}$, steady states (4) and (5) vanish and the stability properties of steady state (3) change (unstable for $D < D_{cr}$ and stable for $D > D_{cr}$). This bifurcation value D_{cr} was analytically found as a function of the two feed substrate concentrations and the model parameters. For the values of the two feed substrate concentrations used in all the simulations: $D_{cr} = 0.50 \text{ h}^{-1}$. Finally, for $D \geq D_{cr}$, steady state (3) vanishes as well and the washout steady state (2) becomes the only linearly stable washout steady state. In summary, for low dilution rates, the system consumes both substrates, but mainly glucose, whereas for high dilution rates, biomass grows exclusively on glucose. The single steady state that is stable is always the one that yields the highest biomass concentration (Figure 4a).

We turn now to the steady-state results for tank 2. Here, the equations of the segregated approach, the unsegregated approach, and the unstructured approach are all different, so in general, three different sets of results will be obtained for this tank. As the preceding discussion indicated, more than one steady state is possible for tank 1 for a given set of operating parameters. Since the steady-state equations for the second tank depend on the steady-state solution for the first tank, it is obvious that there must be at least one solution for the second tank for each solution for the first tank. Thus, there exist multiple steady states for the second tank, as well. However, the more interesting question is how many steady

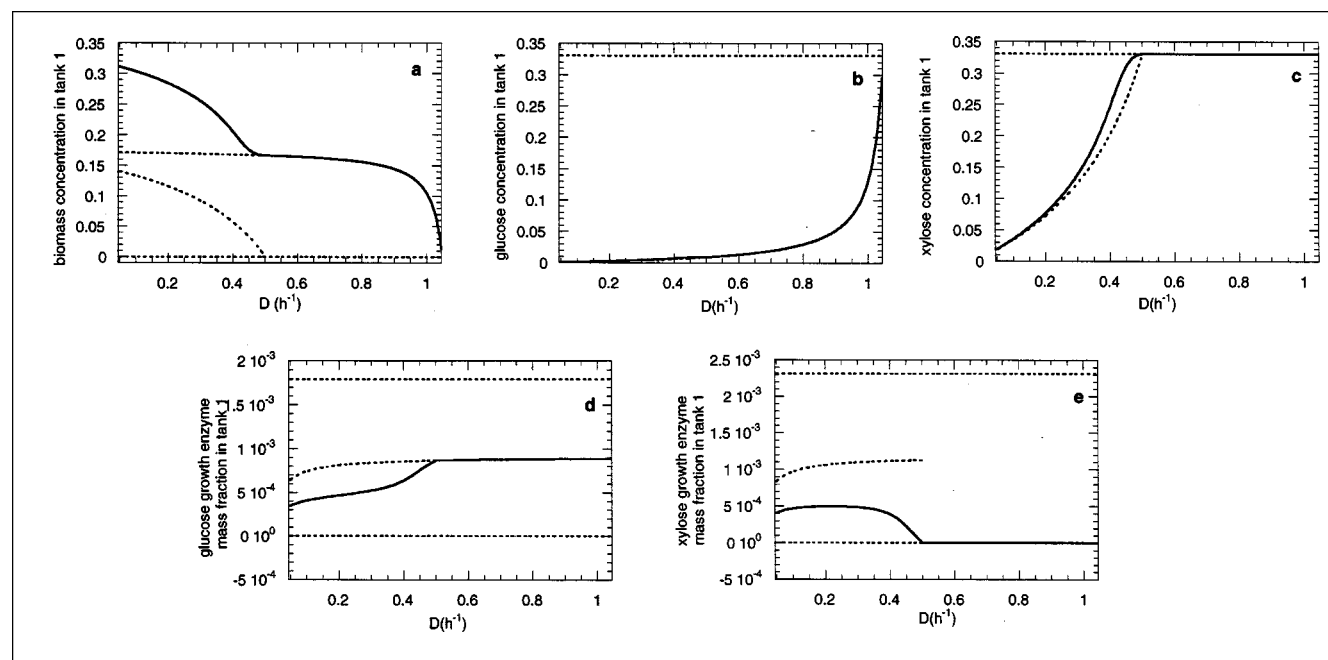


Figure 4. Model of Kompala et al. (1986): five steady-state bifurcation diagrams for tank 1.

Dilution rate D is the bifurcation parameter for $(s_1 r)_{Glu} = (s_1 r)_{Xyl} = 0.33 \text{ kg} \cdot \text{m}^{-3}$. —: Linearly asymptotically stable steady-state solutions; ---: linearly asymptotically unstable steady-state solutions. (a) Biomass concentration; (b) glucose concentration; (c) xylose concentration; (d) glucose growth enzyme mass fraction; (e) xylose growth enzyme mass fraction.

states in tank 2 correspond to each steady state in tank 1. Since, in practice, only stable steady states are observed, we focused on finding how many steady states in tank 2 correspond to each *stable* steady state in tank 1 and then characterizing the stability of these steady states. Also, as already noted, the steady-state equations for the second tank are different for the three modeling approaches considered in this article. Thus, we are also interested in the qualitative and quantitative steady-state differences between these three approaches.

A detailed analysis of the steady-state equations of the unsegregated approach has shown that for $D < D_{cr}$ there exists a unique and stable steady-state solution for tank 2 corresponding to the stable steady-state solution for tank 1. In this steady state both substrates are consumed in tank 2, but the biomass grows primarily on xylose. Thus, according to the unsegregated approach, when biomass grows primarily on glucose in tank 1 (steady state (5)), it continues to consume both substrates in tank 2, but due to the significant reduction of glucose concentration which occurs in tank 1, the biomass in tank 2 grows mainly on xylose. However, a significant qualitative change in the tank 2 steady-state results is observed for dilution rates above the critical bifurcation value D_{cr} but below a second critical value ($0.50 \text{ h}^{-1} = D_{cr} < D < D'_{cr} = 0.95 \text{ h}^{-1}$): there exist two steady states ((3a) and (3b), respectively) for tank 2 corresponding to the stable steady state (3) in tank 1. In the first steady-state situation (3a), both substrates are consumed. Xylose is mainly consumed for $0.50 \text{ h}^{-1} < D < 0.90 \text{ h}^{-1}$, whereas for $0.90 \text{ h}^{-1} < D < 0.95 \text{ h}^{-1}$, glucose is the substrate of primary consumption. The second steady state (3b) corresponds to the case where only glucose is consumed. Throughout this region of dilution rates, steady

state (3a) is linearly stable, whereas steady-state (3b) is linearly unstable. Finally, for $D > 0.95 \text{ h}^{-1}$, steady-state (3a) vanishes and steady state (3b) becomes asymptotically stable. Thus, there exists a region in the dilution rate space ($0.50 \text{ h}^{-1} = D_{cr} < D < D'_{cr} = 0.95 \text{ h}^{-1}$), where there exist *two* solutions, one stable and the other unstable, for the second reactor corresponding to the stable steady-state solution (3) for the first reactor.

The solution of the steady-state equations for the segregated model shows that for $D < D_{cr}$, the situation in tank 2 is qualitatively and quantitatively similar to the steady-state results for tank 2 yielded by the unsegregated approach; that is, a unique and stable steady state exists where both substrates are consumed with xylose being the substrate of primary consumption. Moreover, there is again a region in the dilution rate space where the segregated model has two steady-state solutions corresponding to the stable steady-state solution for the first tank. The lower bound of this region is the same as in the unsegregated model (the bifurcation value D_{cr}). However, the upper bound is lower (0.8 h^{-1}) than the corresponding one for the unsegregated model (0.95 h^{-1}). Again, the first steady state corresponds to the case where both substrates are consumed and it is stable, while in the second steady-state solution, which is unstable, only glucose is consumed. It was shown analytically that this unstable steady-state solution (only glucose is consumed) is identical for both the segregated and unsegregated approaches. For $D > 0.8 \text{ h}^{-1}$, the first steady state (both substrates are consumed) vanishes and the second steady state (only glucose is consumed) becomes stable.

Figure 5 shows the stable steady-state results for tank 2 for all three modeling approaches as a function of the dilution

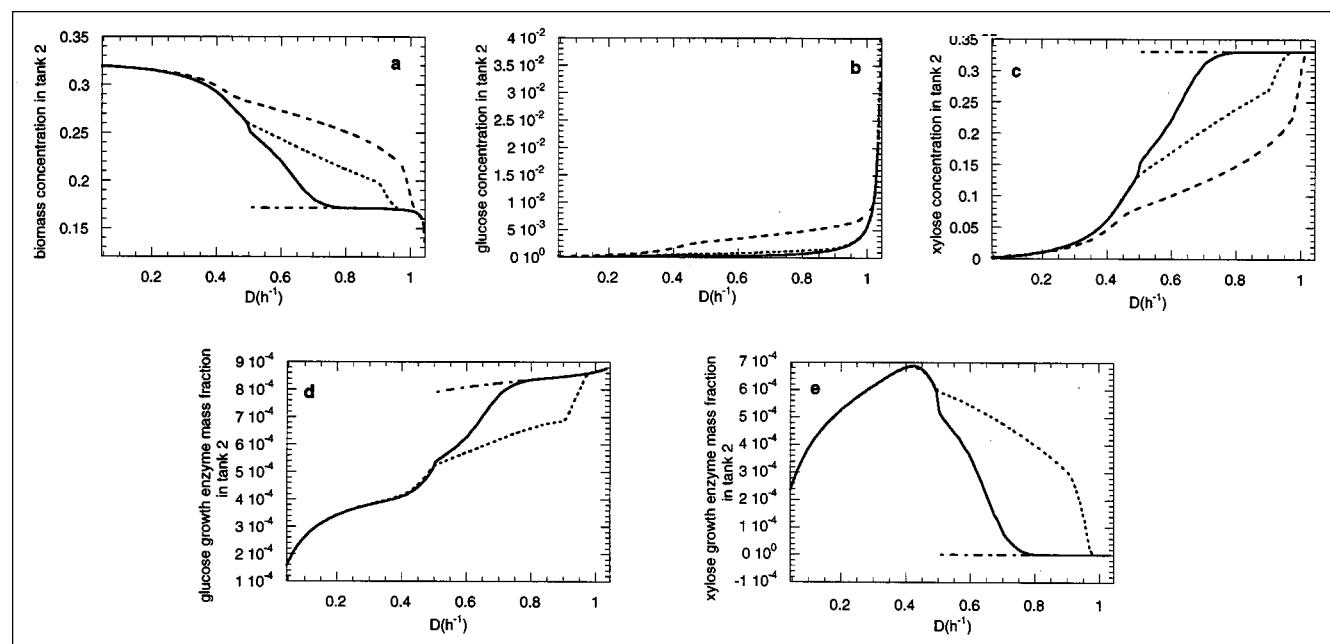


Figure 5. Model of Kompala et al. (1986): steady-state solutions for tank 2.

It corresponds to the stable steady-state solution in tank 1, as a function of the dilution rate D for $(s_1)_f)_{G/Yl} = (s_1)_f)_{X/Yl} = 0.33 \text{ kg} \cdot \text{m}^{-3}$, as predicted by the three models. —: The stable solution of the segregated model; ---: the stable solution of the unsegregated model; — · —: the stable solution of the unstructured model; - - - -: the unstable solution of both the segregated and unsegregated steady-state models. (a) Biomass concentration; (b) glucose concentration; (c) xylose concentration; (d) glucose growth enzyme mass fraction; (e) xylose growth enzyme mass fraction.

rate. The unstable steady-state solution which is identical for the segregated and unsegregated models is also plotted for the entire range of its existence ($D > D_{cr}$). One can make the following observations: (a) For $D < D_{cr}$, the segregated and unsegregated models produce virtually indistinguishable results; (b) in the entire region of the dilution rate parameter space where the unsegregated model has multiple steady-state solutions ($0.50 \text{ h}^{-1} = D_{cr} < D < D'_{cr} = 0.95 \text{ h}^{-1}$), the results of the segregated and unsegregated models exhibit significant differences; (c) for very high dilution rates $D > 0.95 \text{ h}^{-1}$, the two approaches produce identical results; (d) the unstructured model overestimates the biomass and glucose concentrations and underestimates the xylose concentration in the entire region of the parameter space.

As the results presented in Figure 5 show clearly, for values of the dilution rate where the unsegregated model predicts more than one steady-state solution for the second tank corresponding to the stable steady-state solution for the first tank, biomass segregation is important, whereas for dilution rates where there is a unique steady-state solution in tank 2

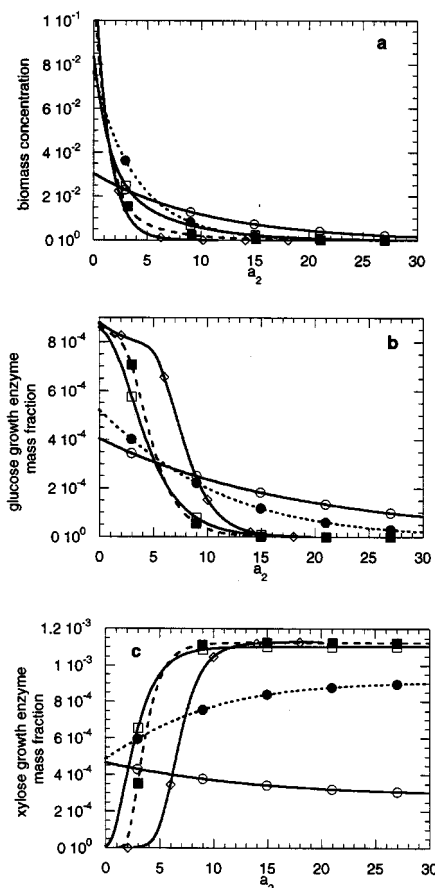


Figure 6. Model of Kompala et al. (1986): steady-state age (time spent in CSTR-2) distributions of the biomass and the mass fractions of the two growth enzymes for different dilution rates.

It was predicted by the segregated model.

—○—○— : $D = 0.1 \text{ h}^{-1}$; —●—●— : $D = 0.3 \text{ h}^{-1}$; —□—□— : $D = 0.5 \text{ h}^{-1}$; —■—■— : $D = 0.7 \text{ h}^{-1}$; —◇—◇— : $D = 0.9 \text{ h}^{-1}$. (a) Biomass concentration; (b) glucose growth enzyme mass fraction; (c) xylose growth enzyme mass fraction.

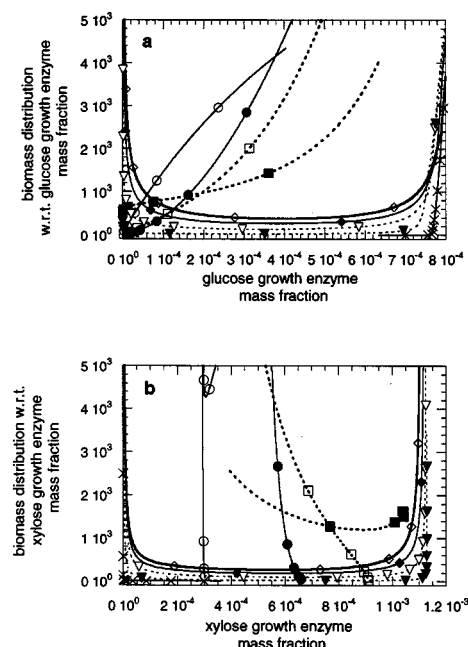


Figure 7. Model of Kompala et al. (1986): steady-state biomass distributions with respect to the mass fractions of the two sets of substrate-utilizing enzymes for different dilution rates.

It was predicted by the segregated model.

—○—○— : $D = 0.1 \text{ h}^{-1}$; —●—●— : $D = 0.2 \text{ h}^{-1}$; —□—□— : $D = 0.3 \text{ h}^{-1}$; —■—■— : $D = 0.4 \text{ h}^{-1}$; —◇—◇— : $D = 0.5 \text{ h}^{-1}$; —◆—◆— : $D = 0.6 \text{ h}^{-1}$; —▽—▽— : $D = 0.7 \text{ h}^{-1}$; —▼—▼— : $D = 0.8 \text{ h}^{-1}$; —*—*— : $D = 0.9 \text{ h}^{-1}$. (a) Biomass distribution with respect to the glucose growth enzyme system; (b) biomass concentration with respect to the xylose growth enzyme system.

corresponding to the stable steady state in tank 1, biomass segregation can be neglected. We infer from this that there must be an association between multiplicity in the steady-state results for the second tank according to the unsegregated approach, and differences between the predictions of the segregated and unsegregated approaches.

An attempt was made to obtain deeper insight into the problem of why the two approaches gave essentially the same prediction in some circumstances and quite different predictions in others. This attempt was based on the results presented in Figures 6, 7 and 8. Figure 6 shows the steady-state distributions with respect to age of biomass concentration and the two elements of the biomass state vector for various dilution rates. Figure 7 shows the steady-state distributions of biomass concentration with respect to the two elements of the biomass state vector for different dilution rates. These graphs were calculated from the results shown in Figure 6 using Eqs. 46 and 74 of the previous article (Mantzaris et al., 1998). Figure 8 shows the coefficients of variation of steady-state biomass distributions with respect to the two elements of the biomass state vector as functions of the dilution rate.

Notice (Figure 6) that the steady-state age distributions of the biomass concentration become steeper and narrower as the dilution rate increases, but they are very broad for low dilution rates. Notice also (Figure 7) the qualitative change in the steady-state biomass distributions with respect to the two

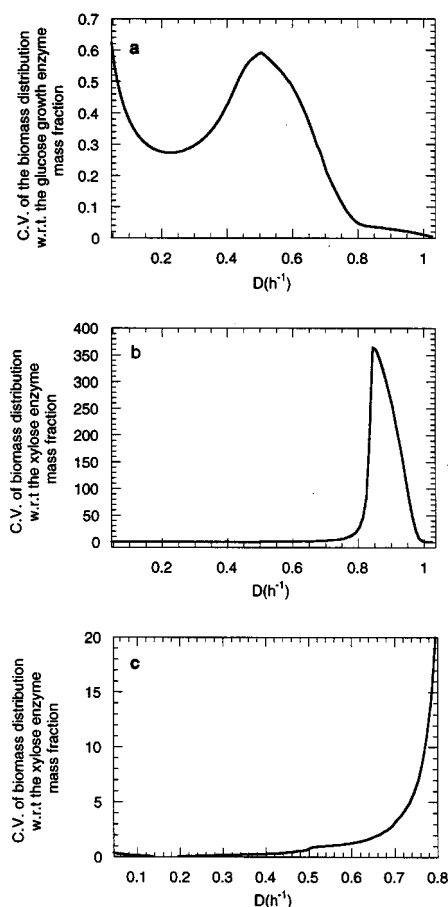


Figure 8. Model of Kompala et al. (1986): coefficient of variation (C.V.) of the two steady-state biomass distributions with respect to the mass fractions of the two growth enzyme systems as functions of the dilution rate D , as predicted by the segregated model.

(a) C.V. of the biomass distribution with respect to the glucose growth enzyme system over the entire range of dilution rates; (b) C.V. of the biomass distribution with respect to the xylose growth enzyme system over the entire range of dilution rates; (c) C.V. of the biomass distribution with respect to the xylose growth enzyme system over the range of dilution rates from 0 – 0.8 h^{-1} .

elements of the state vector that takes place at the bifurcation value $D_{cr} = 0.50 \text{ h}^{-1}$: at dilution rates lower than the critical value the biomass distributions with respect to the two elements of the state vector are unimodal, but they become bimodal at dilution rates higher than the critical. Moreover, as Figure 8 shows, for $0.5 \text{ h}^{-1} < D < 0.8 \text{ h}^{-1}$, both steady-state biomass distributions with respect to the two elements of the state vector are broad (large coefficient of variation). On the other hand, for $D < D_{cr} = 0.50 \text{ h}^{-1}$, the steady-state biomass distribution with respect to the mass fraction of the xylose growth enzyme system is relatively narrow (small coefficient of variation), whereas the corresponding distribution with respect to the mass fraction of the glucose growth enzyme system is broad. Finally, for $D > 0.8 \text{ h}^{-1}$, the steady-state biomass distribution with respect to the mass fraction of the glucose growth enzyme system becomes narrow.

These observations explain, at least at one level of understanding, why the predictions of the segregated and unsegregated approaches agree in some domains of the dilution rate parameter space and disagree in others. To see this, we will divide the dilution rate parameter space into four regions.

(1) For $D < D_{cr} = 0.50 \text{ h}^{-1}$, the unique (corresponding to the stable steady-state solution in the first tank) and stable steady-state solutions of both approaches predict that both substrates are consumed but that biomass grows primarily on xylose. Furthermore, despite the fact that the distributions with respect to age of the biomass and both elements of the biomass state vector are broad (Figure 7), and the functions $f(z_2^1, s_2)$, $g(z_2^1, s_2)$, and $h(z_2^1, s_2)$ of the previous article (Mantzaris et al., 1998) are all nonlinear with respect to the state vector, the biomass distribution with respect to the mass fraction of xylose growth enzyme system is narrow (Figure 8). At low dilution rates, therefore, the biomass in the second tank is nearly homogeneous insofar as the mass fraction of the xylose enzyme system is concerned, and since xylose is the substrate of primary consumption, the biomass behaves as if it were entirely homogeneous insofar as its growth and nutrient uptake rates are concerned. Thus, the differences between the predictions of the two approaches are minimal or nonexistent.

(2) For $0.50 \text{ h}^{-1} < D < 0.80 \text{ h}^{-1}$, the *stable* steady-state solutions of both the segregated and unsegregated models predict that both substrates are consumed. Moreover, according to the segregated model, both steady-state biomass distributions with respect to the elements of the state vector are broad (large coefficients of variation, as Figure 8 shows) and the functions $f(z_2^1, s_2)$, $g(z_2^1, s_2)$, and $h(z_2^1, s_2)$ are nonlinear with respect to the state vector. As a result, the predictions of the segregated and unsegregated approaches are quite different, since in this region, biomass is inhomogeneous with respect to all important parameters.

(3) For $0.80 \text{ h}^{-1} < D < 0.95 \text{ h}^{-1}$, the segregated model has a unique steady state (corresponding to the stable steady-state solution in the first tank) where only glucose is consumed. For this type of steady state, the functions $f(z_2^1, s_2)$, $g(z_2^1, s_2)$, and $h(z_2^1, s_2)$ are all linear with respect to the state vector and also, as Figure 8 shows, the steady-state biomass distribution with respect to the mass fraction of the glucose growth enzyme system is narrow. Thus, one would expect that in this region of the parameter space, the segregated and unsegregated approaches should produce identical results. However, as discussed earlier, the unsegregated model has in this region two steady-state solutions corresponding to the stable steady-state solution in the first tank. The steady state where only glucose is consumed is linearly unstable for the unsegregated approach. Thus, in this region of the parameter space, the unsegregated model asymptotically approaches the stable steady state where both substrates are used. Hence, despite the fact that the steady-state solution predicted by the segregated model exists also for the unsegregated model, its lack of stability for the latter model results in the observed differences between the two approaches.

(4) For $0.95 \text{ h}^{-1} < D < D_u = 1.045 \text{ h}^{-1}$, both the segregated and unsegregated models have a unique steady state (corresponding to the stable steady state in the first tank) where only glucose is consumed. For this type of steady state,

the functions $f(z_2^1, s_2)$, $g(z_2^1, s_2)$, and $h(z_2^1, s_2)$ are all linear with respect to the state vector, and so the two approaches produce identical steady-state results as shown in Figure 6.

A more complete discussion of the steady-state problem including the mathematical proofs of all the statements made throughout this section can be found elsewhere (Mantzaris, 1999).

Second Example: Transient Simulations

Figures 9 and 10 present the results of the comparison between the three models for a transient simulation performed with $D = 0.8 \text{ h}^{-1}$. This dilution rate value was chosen with the intention of examining the transient behavior for a case where the three models exhibit large steady-state differences. The same initial conditions were used for all three models.

In the first reactor (Figure 9), the predictions of all three approaches asymptotically approach the same steady state, as expected. Also, there is a perfect agreement between the segregated and unsegregated approaches, since the corresponding equations are identical. However, the dynamic response to the unstructured model exhibits large differences when compared to the results of the other two models. This is because the unstructured model, by construction, does not take into account the influence of the change of environmental conditions on the states.

In the second reactor (Figure 10), the unsegregated approach predicts two growth phases. During the first phase, where the glucose concentration is high, biomass grows on glucose. After glucose becomes practically depleted, the unsegregated model predicts a large lag phase, during which the system prepares for the consumption of the slow substrate (xylose) by increasing the mass fraction of the xylose growth

enzyme. Finally, during the second growth phase, the system grows exclusively on xylose. On the contrary, the segregated model does not predict a second growth phase on xylose. Such an “exclusive” growth on xylose predicted by the unsegregated model is not possible, since there *necessarily* exists a significant part of biomass (the “young” biomass just entering the second reactor) which requires a certain amount of time in order to adjust to the conditions in the second tank. These conditions are vastly different from the corresponding ones in the first tank where practically all biomass grows on glucose. This is a typical situation where neglecting biomass segregation can lead to results which are not only quantitatively but also qualitatively wrong. Notice also that the unstructured model qualitatively produces similar results to the unsegregated model (two growth phases separated by a lag phase), but it overestimates the biomass and glucose concentrations and underestimates the xylose concentration.

Comments on Second Example

An important point revealed by the results presented is that, at a given set of operating conditions, the stabilities of corresponding steady states of the segregated and unsegregated approaches may not be the same. Thus, at higher dilution rates, the segregated approach has the steady state where only glucose is used as the stable one and the steady state where both glucose and xylose are used as the unstable one. The unsegregated approach reverses this prediction, and because of this, the predictions of the two approaches show substantial differences.

Differences in the predictions of the two approaches occur even when corresponding steady states of the two approaches have the same stabilities, however. An interesting feature of

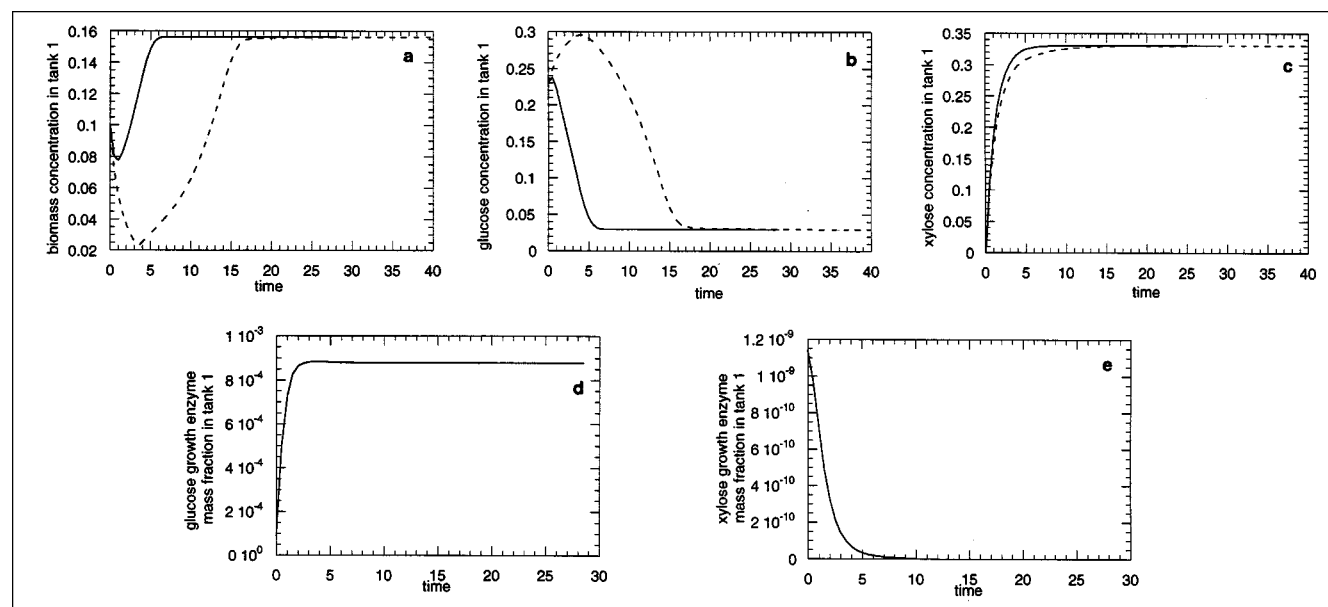


Figure 9. Model of Kompala et al. (1986): Tank 1.

A transient simulation: $D = 0.8 \text{ h}^{-1}$, $(s_1)_G|u = (s_1)_X|l = 0.33 \text{ kg} \cdot \text{m}^{-3}$. —: Segregated and unsegregated models; ---: unstructured model. (a) Biomass concentration; (b) glucose concentration; (c) xylose concentration; (d) glucose growth enzyme mass fraction; (e) xylose growth enzyme mass fraction.

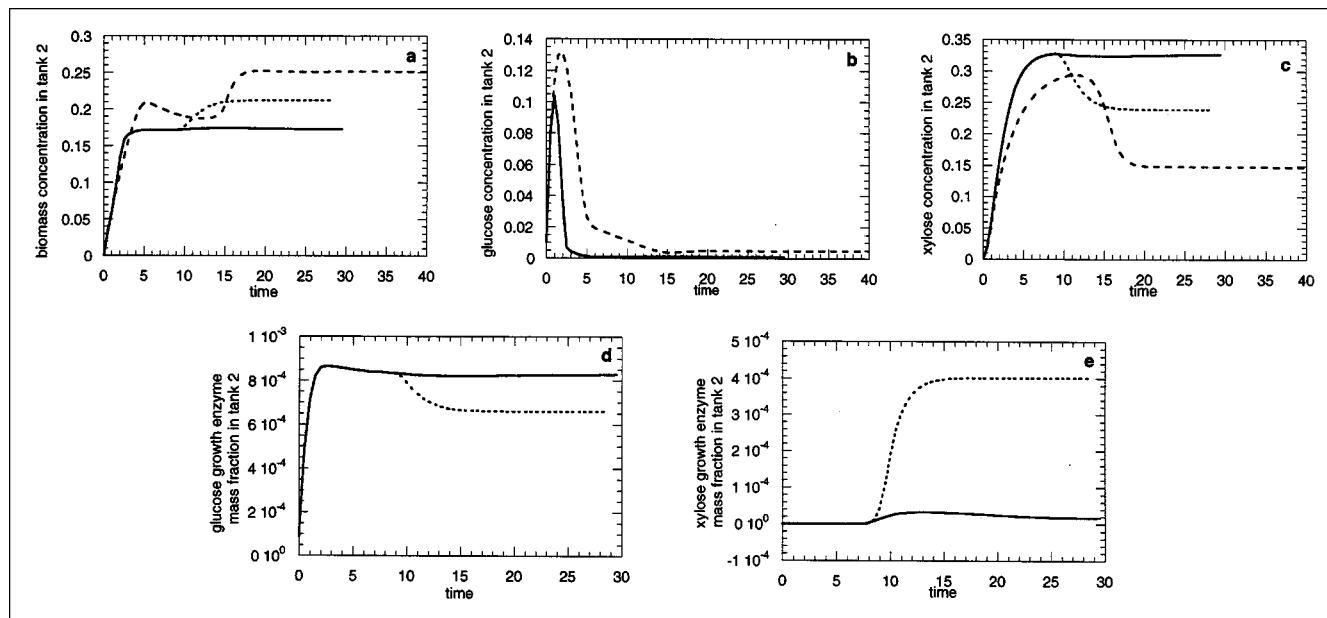


Figure 10. Model of Kompala et al. (1986): Tank 2.

A transient simulation: $D = 0.8 \text{ h}^{-1}$, $(s_{1f})_{Glucose} = (s_{1f})_{Xylose} = 0.33 \text{ kg} \cdot \text{m}^{-3}$. —: Segregated model; ---: unsegregated model; — · —: unstructured model. (a) Biomass concentration; (b) glucose concentration; (c) xylose concentration; (d) glucose growth enzyme mass fraction; (e) xylose growth enzyme mass fraction.

the results just presented is that differences between the segregated and unsegregated modeling approaches are associated with the occurrence of multiplicity in the second reactor (existence of more than one steady state in the second reactor for a single steady state in the first reactor). We examined this further by considering a very simple structured model proposed by Roels (1983). The model is nonlinear and it always has two steady states in the first reactor, only one of which is stable. It was shown analytically that only one steady state in the second reactor is associated with the stable steady state in the first reactor, and in addition, numerical simulations showed that the differences between the predictions of the segregated and unsegregated modeling approaches are negligible in this case. It was shown in the previous article (Mantzaris et al., 1998) that the segregated and unsegregated approaches will make identical predictions for the biomass concentration and the mean values of the abiotic environment and biomass state vectors in the second tank if the kinetic expressions of the model are linear in the state vector of the biomass. The kinetic expressions of the Roels model are never linear in the state vector, and so the agreement of the two approaches cannot be attributed to such linearity. This is another bit of evidence that supports the conclusion that differences between the predictions of the two approaches are somehow associated with multiplicity in the second tank. Unfortunately, we have been unable to produce a proof of this conclusion nor do we understand why it is so, if it is so.

Discussion and Conclusions

The results described above show that the predictions of the unsegregated version of a structured model for what hap-

pens in the second tank of a cascade are sometimes but not always appreciably different from the predictions of the segregated version of the model. Therefore, segregation of biomass is an important feature of the system in some circumstances but not in others.

Clearly, it is desirable to have some means to predict when segregation is important and when it is not. Unfortunately, we have been unable to provide a complete and clear-cut method for making such a prediction. It was shown theoretically that the predictions of the two versions will be the same insofar as mean quantities are concerned if the production and uptake rate vectors of the model used are linear in the state vector. However, the computational results show that such linearity is not necessary for the predictions to be the same or nearly the same: the two versions can make the same predictions even when they are both highly nonlinear. We have stated what we believe to be the reasons why the segregated and unsegregated versions of the model of Kompala et al. (1986) make the same predictions under certain conditions where both versions are highly nonlinear, but these statements were made only after rather extensive calculations had been done and much thought had been given to the results obtained. If a different model were to be used, and if it was nonlinear, we expect that similar calculations would have to be done to find out the conditions, if any, where the unsegregated version of the model would predict the same thing as the segregated version.

The conclusion to be drawn from this is that, if one has a structured model that works well for a single tank, one might as well use the segregated version of the model to predict what is going to happen in the second tank because one does not know the conditions (aside from linearity) that are sufficient for its segregated and unsegregated versions to predict

the same things for the second tank. One must solve partial differential equations instead of ordinary differential equations when the segregated version of a model is used, but the experience gained in obtaining the results presented herein suggests that this need not be an overwhelming difficulty.

This does not mean that the unsegregated approach to modeling what happens in the second tank is worthless. If it could be proved that disagreement between the segregated and unsegregated approaches occurs if and only if the equations for the second tank exhibit multiplicity, and if analysis showed that the equations of the unsegregated approach did not exhibit multiplicity, then the ordinary differential equations of the unsegregated approach could be used to predict the behavior of the second tank correctly. In addition, one expects that the trial-and-error calculations involving the more complicated equations of the segregated approach will be required in, say, attempts to optimize the performance of a cascade of bioreactors. Reasonably accurate estimates of system behavior will be needed to start the calculations, and these can be obtained using the unsegregated version of a structured model.

Unstructured models may be disposed of more briefly. If a structured model in which one has confidence is available, there is no point in expending the effort necessary to construct the unstructured version of that model, for it must necessarily fail in transient situations and it will fail even in many steady-state situations in the second tank of a cascade. Unstructured models should be used only as a last resort, when nothing better is available, and when they are used, one must not expect them to give anything more than a very rough idea

of what may happen in a transient bioreactor or in the second tank of a bioreactor cascade.

Acknowledgments

N. V. Mantzaris was supported by funds provided by the National Science Foundation under grant No. BES 9319380; he thanks the Foundation for its support. A. G. Fredrickson was a Visiting Professor at the International Center for Cooperative Research in Biotechnology (ICBiotech) at Osaka University in Osaka, Japan when the bulk of the research reported herein was done. He is grateful to the authorities of ICBiotech for their support during his stay in Osaka.

Literature Cited

- Bentley, W. E., R. H. Davis, and D. S. Kompala, "Dynamics of Induced CAT Expression in *E. Coli*," *Biotechnol. Bioeng.*, **38**, 749 (1991).
- Bentley, W. E., and D. S. Kompala, "A Novel Structured Kinetic Modeling Approach for the Analysis of Plasmid Instability in Recombinant Bacterial Cultures," *Biotechnol. Bioeng.*, **33**, 49 (1989).
- Kompala, D. S., D. Ramkrishna, N. B. Jansen, and G. T. Tsao, "Investigation of Bacterial Growth on Mixed Substrates. Experimental Evaluation of Cybernetic Models," *Biotechnol. Bioeng.*, **28**, 1044 (1986).
- Mantzaris, N. V., PhD Thesis, University of Minnesota, in press (1999).
- Mantzaris, N. V., P. Daoutidis, F. Sienic, and A. G. Fredrickson, "Growth Processes in a Cascade of Bioreactors: Mathematical Models," *AIChE J.*, in press (1998).
- Roels, J. A., *Energetics and Kinetics in Biotechnology*, Elsevier, Amsterdam, p. 272 (1983).

Manuscript received July 9, 1998, and revision received Oct. 13, 1998.